Excited-State Double Proton Transfer of 7-Azaindole in Water Nanopools

Oh-Hoon Kwon and Du-Jeon Jang*

School of Chemistry, Seoul National University, NS60, Seoul 151-742, Korea

Received: June 13, 2005; In Final Form: August 29, 2005

The excited-state proton-transfer dynamics of 7-azaindole occurring in the water nanopools of reverse micelles has been investigated by measuring time-resolved fluorescence spectra and kinetics, as well as static absorption and emission spectra, with varying water content and isotope. 7-Azaindole molecules are found to exist in the bound-water regions of reverse micelles. The rate constant and the kinetic isotope effect of proton transfer are smaller than those in bulk water although both increase with the size of the water nanopool. The retardation of proton transfer in the bound regions is attributed to the increased free energy of prerequisite solvation to form a cyclically H-bonded 1:1 7-azaindole/water complex.

I. Introduction

Proton transfer has been attracting considerable attention because it plays a key role in a wide variety of biological and chemical phenomena such as water autoionization, fast proton diffusion, acid−base reactions, DNA mutagenesis, enzyme catalysis, and proton pumps.[1−6] In particular, tautomerization through bridging H-bonds is an example of proton-transfer processes in biological systems. Proton transfers of 7-azaindole (7AI) and its dimers, structurally similar to H-bonded DNA base pairs, have been studied extensively.[4,7−13] 7AI is a chromophoric moiety of 7−azatryptophan, a novel in situ optical probe for the structures and dynamics of proteins.[14] The photochemistry and the photophysics of 7AI have been widely investigated in a variety of environments,[4,7−27] since the first observation of its excited-state double proton transfer (ESDPT) in 1969.[7] Metal−7AI complexes have potential applications in electroluminescent devices as well.[28]

Solvent involvement in the tautomerization of 7AI in water and alcohols has attracted considerable attention.[15−25] In particular, the two-step model of Scheme 1 involving water or alcohols (ROH) has been widely discussed.[17−22] The first step is solvent reorganization (k_1) to form a cyclically H-bonded 7AI/ROH complex, and the second step is intrinsic proton transfer (k_{pt}) catalyzed by the complexed solvent molecule. In one limit, solvent reorganization can be the rate-limiting step so that the observed rate constant (k_{PT}) becomes k_1. In the opposite limit, that the equilibrium (k_1/k_{-1}) between solvent reorganization and solvent randomization (k_{-1}) is rapid relative to k_{pt}, k_{PT} is independent of solvent dynamics and is expressed as (k_1/k_{-1})-k_{pt}. The static role of solvation is also reported to be $k_{PT} = k_{pt}\exp(-\Delta G^{\ddagger}/k_B T)$ in the manner of the transition-state theory,[19] where $\Delta G^{\ddagger}$ is the free energy of formation for a cyclically bridged 1:1 complex ($N^{\ddagger}$). Solvation to achieve an appropriate configuration is generally believed to be prerequisite to efficient proton tunneling.[17−24]

Because water is indisputably the most important medium for biological processes to occur, it is necessary to investigate biologically important processes closely in biologically relevant aqueous systems. Reverse micelles are interesting systems to be explored because they can serve not only as nanoreactors

SCHEME 1: Two-Step Model for the ESDPT of 7AI in Water or Alcohols

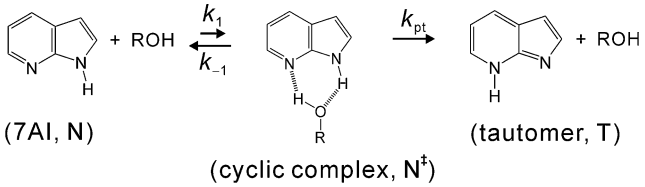

but also as simple biological models. Reverse micelles in hydrocarbon solvents formed by surfactant molecules having polar headgroups pointing inward are good mimic systems for the exploration of biological membranes and biologically confined water molecules.[29−32] A distinguished feature of reverse micelles is their ability to make nonpolar solvents solubilize a large amount of water in their inner polar cores.[33] The water nanopools resemble the water pockets often found in various bioaggregates such as proteins, membranes, and mitochondria. Because the physical and the chemical properties of solvent water and solutes confined in a reverse micelle can be controlled by changing the size of its core water nanopool, the characterization and the exploitation of reverse-micellar systems have been carried out greatly.[34−39] About 20 molecules of surfactant Aerosol-OT (sodium 1,4-bis-2-ethylhexylsulfosuccinate, AOT) form a reverse micelle having a radius of 1.5 nm above the critical concentration of 1 mM in a hydrocarbon solvent.[33] The gradual addition of water to the AOT solution forms microemulsions of nanometer-sized water droplets surrounded by AOT molecules. In *n*-heptane, the radii in nanometers of the water pools are about $0.15w_0$ where w_0 is the molar ratio of water to AOT.[40] Water molecules at interfacial peripheries are strongly bound to the polar or ionic headgroups of surfactant molecules while those at micellar cores are relatively free.[29] Thus, water confined in reverse micelles is known to have characteristic properties that are distinctively different from those of bulk water.

The structures of AOT reverse micelles have been extensively studied using various spectroscopic methods of NMR, IR, and Raman.[40−46] The solvation dynamics and the dielectric relaxation of water inside reverse micelles have also been studied by using time-resolved fluorescence Stokes-shift spectroscopy, terahertz electric-field spectroscopy, and molecular dynamics simula-

* To whom correspondence should be addressed. E-mail: djjang@snu.ac.kr.

10.1021/jp053187v CCC: $30.25
Published on Web 10/04/2005

tions.[47−57] It is reported that water molecules inside reverse micelles are roughly classified into two types, "bound water" and "free water".[29−31] On one hand, bound water molecules in the interfacial peripheries of water nanopools are immobile because of strong binding to the polar headgroups of AOT molecules. On the other hand, free water molecules in the central areas of reverse micelles have been suggested to be mobile almost like bulk water molecules. Thus, bound water molecules are often considered as "biological water" present in the immediate vicinity of biomolecules.[58] Although excited- and ground-state acid−base reactions in reverse micelles were investigated,[32,59,60] solvent-assisted proton-transfer dynamics has not been studied in aqueous reverse micelles yet to our knowledge. We note that the luminescence properties of 7AI in aqueous reverse micelles have also been reported.[27]

In this paper, we report the solvation dynamics and the proton transfer of excited 7AI in the water nanopools of AOT reverse micelles. We have focused our research on understanding the unusual properties of confined water molecules and the relation of solvent motion and proton transfer because molecules in the water nanopools of reverse micelles behave differently from those in bulk water.

II. Experimental Section

7AI (99%), *n*-heptane (anhydrous), and ^2H_2O (isotopic purity ≥ 99.9%) were used as purchased from Sigma-Aldrich. Water (>18 MΩ/cm) was triply distilled while AOT (>99%, Sigma-Aldrich) was dried over molecular sieves (4 Å, Merck). 7AI-dissolved AOT micelles, having 0.05 7AI molecule per micelle in average, were prepared by adding 2×10^{-5} mol of 7AI to a 100-mL solution of 0.09-M AOT in *n*-heptane. The concentration of 7AI was kept at 2×10^{-4} M in all our samples except cyclohexane solutions, where it was 1×10^{-5} M. The w_0 value was adjusted by adding water to the 7AI-dissolved AOT micelles several hours later. All our reverse-micellar samples were transparent and monodisperse.

Absorption spectra were obtained by using a spectrophotometer (Scinco, S-2040) while fluorescence spectra were measured with a fluorimeter having a 75-W Xe lamp (Acton Research, XS432), a 0.30-m monochromator (Acton Research, Spectrapro-300), and a photomultiplier tube (Acton Research, PD438) following excitation at 288 nm. An actively/passively mode-locked 25-ps Nd:YAG laser (Quantel, YG701) and a 10-ps streak camera (Hamamatsu, C2830) attached to a CCD detector (Princeton Instruments, RTE128H) were employed for the excitation and the detection of time-resolved emission measurements, respectively. Samples were excited with 288-nm pulses generated through a Raman shifter filled with methane at 10 atm and pumped by the fourth-harmonic pulses (266 nm) of the laser. Emission wavelengths were selected by an appropriate combination of band-pass and cutoff filters for kinetics measurements or by a 0.15-m monochromator (Acton Research, Spectrapro-150) for recording transient spectra. Time-resolved fluorescence spectra were constructed by measuring fluorescence decay kinetics every 5 nm. Fluorescence kinetic constants were extracted by fitting profiles measured at room temperature to computer-simulated exponential curves convoluted with instrumental response functions having a fwhm of 80 ps. Both static and time-resolved fluorescence spectra were not corrected for the wavelength-dependent sensitivity variation of the detectors.

All our static and time-resolved measurements were carried out at room temperature. Our spectroscopic and kinetic results indicate that practically all of the molecules of 7AI exist within AOT micelles. In neat *n*-heptane, the normal fluorescence of 7AI decays on the time scale of 1600 ps, while the emission of the tautomers, presumably generated from 7AI dimers, decays in 3600 ps. None of these lifetimes have been observed in our AOT-added *n*-heptane samples.

TABLE 1: Spectral Parameters of 7AI in Various Solvents

medium	w_0	λ_{max}^{abs} (nm)	λ_{max}^{em} (nm)	emission quantum yield
cyclohexane	N/A	284	325	0.22[a]
diethyl ether	N/A	286	345	0.31[a]
acetonitrile	N/A	286	360	0.38[a]
methanol	N/A	288	371, 500	0.010,[a] 0.0024[a]
^1H_2O	N/A	289	391	0.032[a]
^2H_2O	N/A	289	391	0.12[a]
^1H_2O in reverse micelles	0	288	350	0.42[b]
	1	288	354	0.35[c]
	4	288	360	0.11[c]
	8	288	363	0.058[c]
	20	288	367	0.039[c]
	60	288	369	0.036[c]

[a] From ref 18. [b] From ref 27. [c] Calculated by multiplying the emission quantum yield at $w_0 = 0$ with I/I_0, where I_0 is fluorescence intensity at $w_0 = 0$.

III. Results and Discussion

Absorption and Emission Spectra. The wavelengths at the absorption maximum (λ_{max}^{abs}) of 7AI in various media (Table 1) suggest that the lowest absorption band of 7AI is spectrally almost insensitive to media. However, the wavelengths at the emission maximum (λ_{max}^{em}) and the emission quantum yields of 7AI show that the emission of 7AI is spectrally sensitive to solvents to a great extent. 7AI molecules at high concentrations in nonpolar aprotic solvents such as cyclohexane are known to form doubly H-bonded dimers and to undergo ESDPT giving tautomeric emission with the maximum at 480 nm.[7−9] 7AI at a very low concentration shows only monomeric normal emission with the maximum at 325 nm. Both the wavelength and the quantum yield of normal emission increase with the polarity of aprotic solvents (Table 1). Two close-lying excited states of ^1L_a and ^1L_b in the chromophore of indole are suggested to give strong fluorescence at high polarity.[61] On one hand, 7AI in methanol exhibits a new emission band at 500 nm besides the normal emission band. Furthermore, the quantum yield of emission from the normal species (N) is remarkably small despite the high polarity of methanol. This has been already attributed to the facile proton transfer of N to form its tautomer (T) following the formation of cyclically H-bonded 1:1 complexes with methanol molecules.[7,15−18] Similar spectral behaviors are also observed in water. While the normal emission band is further shifted to 391 nm due to the high polarity of the solvent, its quantum yield is three times as high as that in methanol, implying that ESDPT possibly occurs in water (vide infra). However, there is no perceivable band of tautomeric fluorescence.[18,25] Although there were controversies on the interpretation of photophysical behaviors in water due to lack of a tautomeric band,[18,25] excited N is now known to undergo ESDPT definitely to form T.[22] Because T* relaxation is even much faster than ESDPT to form T*, tautomeric emission is not observable.[18,22]

As displayed in Figure 1, the lowest absorption band of 7AI in AOT reverse micelles is spectrally insensitive to the addition of water. Interesting changes are noticeable in the emission spectra of 7AI. 7AI in AOT reverse micelles having no water shows a single emission band with the maximum at 350 nm

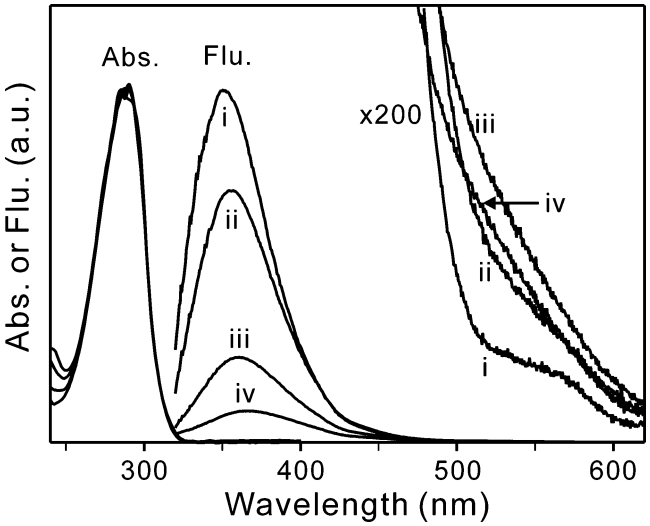

Figure 1. Absorption and fluorescence spectra of 7AI in AOT reverse micelles having $w_0 = 0$ (i), 1 (ii), 4 (iii), and 20 (iv).

and a high quantum yield of 0.42. This suggests that the polarity of AOT reverse micelles at $w_0 = 0$ is comparable with that of ether or acetonitrile (Table 1).[27]

The maximum of normal fluorescence in AOT reverse micelles shifts to low energy gradually with the addition of water. The emission decreases markedly with the water addition to show its quantum yield at $w_0 = 60$ close to that in bulk water, indicating that its quantum yield decreases with a polarity increase. Magnified red tails exhibit that the decrease of normal emission with water addition is followed by the concurrent increase of a green-to-yellow emission, which corresponds to the fluorescence of T* converted from 7AI molecules 1:1 complexed cyclically with water molecules.[23] These spectral changes with w_0 suggest that the proton transfer of N* to form T* is also active in the water pools of reverse micelles as reported in bulk water.[18] Note that the normal emission of 7AI in reverse micelles having a practically highest w_0 value of 60 is shorter in wavelength and greater in intensity than that in bulk water. This implies that the environment of 7AI in reverse micelles even at $w_0 = 60$ is less polar than that in bulk water. Free water in AOT reverse micelles is reported to be very similar to bulk water.[30] Thus, it is probable that 7AI molecules reside in the bound-water regions of the reverse micelles (vide infra). This suggestion is in accordance with the report that the polarity of the local environment of 7AI in AOT reverse micelles is much lower than that of bulk water.[27] Also, it should be noticed that 2-naphthol is present in the "headgroup regions" of reverse micelles, whereas its singly charged anionic derivative is present in the bound regions.[60] Moreover, its multiply charged anionic derivative dissolves in the free-water regions due to electrostatic repulsion by the anionic headgroup of the surfactant.[32,59,60]

Time-Resolved Emission. The time-resolved spectra of Figure 2 reveal that normal fluorescence shifts to the red and that tautomeric fluorescence grow with time in reverse micelles to give a band perceivable at a delay of 1600 ps. The rise of tautomer fluorescence also supports that N* undergoes ESDPT in the water nanopools of AOT reverse micelles. On the other hand, the bathochromic shift of normal emission with time is due to the reequilibration of solvent molecules surrounding photoexcited 7AI molecules. The dipole moment of 7AI has been reported to increase markedly upon excitation.[18]

The time-dependent spectral shift of fluorescence provides a direct measurement of solvation kinetics occurring in the water pools of reverse micelles. Solvation dynamics has often

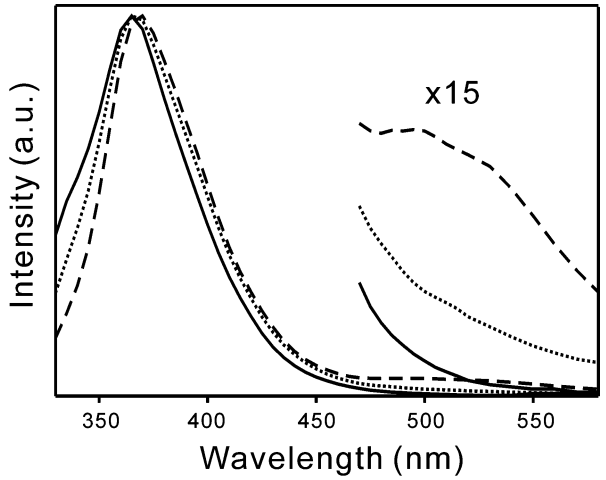

Figure 2. Peak-normalized time-resolved fluorescence spectra of 7AI in AOT reverse micelles having $w_0 = 12$ at delays of 0 (solid), 400 (dotted), and 1600 (dashed) ps from excitation.

been investigated by using the normalized spectral-shift correlation function of $C(t)$, defined as

$$C(t) = \frac{\upsilon(t) - \upsilon(\infty)}{\upsilon(0) - \upsilon(\infty)} \quad (1)$$

The $\upsilon(t)$, $\upsilon(0)$, and $\upsilon(\infty)$ of eq 1 are fluorescence frequencies at time delays of t, 0, and ∞, respectively, after photoexcitation. We have estimated $\nu(0)$ and $\upsilon(t)$ from averaged frequencies at the $^3/_4$ maxima of fluorescence. On the other hand, $\upsilon(\infty)$ was estimated by fitting experimental data to a biexponential function.[62] The bound water of AOT reverse micelles near the hydrophilic interface is very unlikely to show a fast solvation process because of orientational constraints. An AOT reverse micelle is supposed to have a series of environmentally different water domains. The properties of the domains depend on distances from the interface of the micelle exerted on diverse properties of molecules therin.[63] Because most multiple exponential functions can be fitted to a biexponential within a usual margin of experimental error, our $C(t)$ curves were fitted biexponentially.

Each of the $C(t)$ kinetic profiles of 7AI fluorescence in AOT reverse micelles monitored with our temporal resolution of 80 ps shows two decay components (Figure 3). Table 2 shows that the fractional initial amplitudes remain constant with w_0 variation. This agrees with the above suggestion that practically all the 7AI molecules reside in the bound-water regions of AOT reverse micelles. Although solvation time constants decrease with w_0, they are much larger than those expected in free or bulk water.[62] Furthermore, our observed solvation values are much shorter than the solvation time of coumarin 152 located at the headgroup regions.[51b] These also suggest that 7AI exists in the bound-water regions. Fast solvation in the large micelles having headgroups of low density is inferred to originate from the mobility increase of solvent molecules. The fractional amplitudes of two solvation decay components do not change with w_0 variation. We suggest that this comes from two different orientations of 7AI molecules toward the headgroup regions. If the prototropic groups of 7AI point outward, solvent molecules between 7AI molecules and the headgroup regions are considered to be slow in motion to yield the large time constant. The averaged solvation time comparable to the ESDPT time of 7AI suggests that solvent motion monitored with our limited temporal resolution is the slow reorientation of solvent molecules (vide infra).

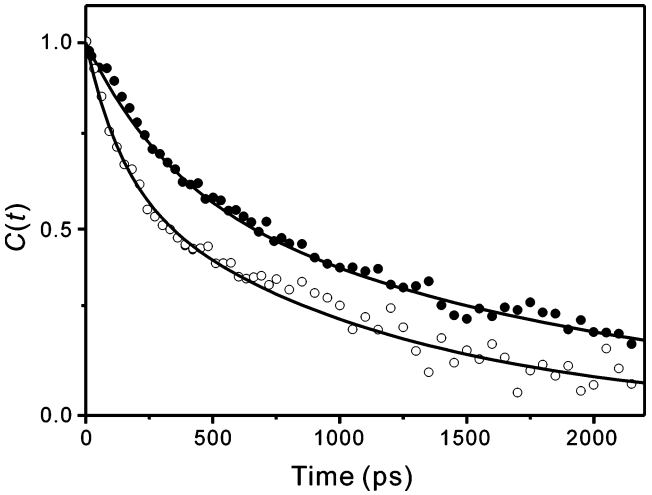

Figure 3. Decay profiles for the $C(t)$ of 7AI fluorescence in AOT reverse micelles having $w_0 = 12$ (closed) and 60 (open). The solid lines denote best-fitted biexponential decays.

TABLE 2: Solvation Time Constant of 7AI in AOT Reverse Micelles, Obtained from Figure 3

w_0	$\Delta\nu$ (cm^{-1})	time (ps)	average time (ps)
12	580	330 (0.36)[a] + 1900 (0.64)	1330[b]
60	680	140 (0.36) + 1100 (0.64)	750[b]

[a] Initial amplitude fraction. [b] Calculated from $\Sigma\tau_i A_i$, where τ and A are the time and the amplitude of each component, respectively.

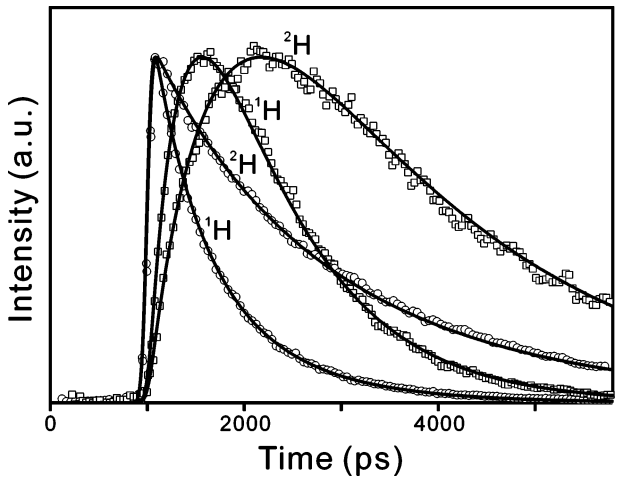

Figure 4. Fluorescence kinetic profiles, monitored at 360 (circles) and ≥550 (squares) nm, of 7AI in reverse micelles of ^1H_2O (^1H) and ^2H_2O (^2H) having $w_0 = 32$. Lines are best-fitted kinetic curves.

The total Stokes shifts of 7AI fluorescence in reverse micelles were observed to be 580 and 680 cm^{-1} at $w_0 = 12$ and 60, respectively. These values are close to the reported values of 500 and 700 cm^{-1} for 7AI in the cosolvent systems of H_2O/ether and H_2O/acetonitrile, respectively.[18] We infer that the band structure of T* fluorescence was observable owing to the small Stokes shift of N* fluorescence in AOT reverse micelles.

Fluorescence Kinetics. For 7AI in the reverse micelles of $w_0 = 32$, fluorescence at a monitored wavelength (λ_{mon}) of 360 nm shows a biexponential decay profile comprised of 470 (63%) and 1080 (37%) ps, while that at ≥550 nm rises within 400 ps and decays on the time scale of 940 ps (Figure 4). On the other hand, the decay times of N* are 1000 (33%) and 2400 (67%) ps with the protic hydrogen of ^2H, while the rise and the decay times of T* are 800 and 2300 ps, respectively, showing remarkable kinetic isotope effects (KIE). We have obtained

TABLE 3: Fluorescence Kinetic Constants of 7AI in AOT Reverse Micelles

w_0	isotope	λ_{mon} (nm)	rise time (ps)	decay time (ps)
0	^1H	360	instant	6200
4	^1H	360	instant	580(38%)+ 1500(62%)
		≥550	0600	1400
	^2H	360	instant	1400(20%) + 3000(80%)
		≥550	1160	2900
8	^1H	360	instant	600(56%) + 1240(44%)
		≥550	0500	1130
	^2H	360	instant	1330(23%) + 2600(77%)
		≥550	0980	2500
16	^1H	360	instant	500(62%) + 1120(38%)
		≥550	0420	1050
32	^1H	360	instant	470(63%) + 1080(37%)
		≥550	0400	940
	^2H	360	instant	1000(33%)+ 2400(67%)
		≥550	0800	2300
60	^1H	360	instant	480(61%) + 1080(39%)
		≥550	0400	950

TABLE 4: Wavelength-Dependent Fluorescence Kinetic Constants of 7AI in AOT Reverse Micelles Having $w_0 = 12$

λ_{mon} (nm)	decay time (ps)
330	210(55%) + 550(45%)
350	460(59%) + 800(41%)
370	550(60%) + 1150(40%)

SCHEME 2

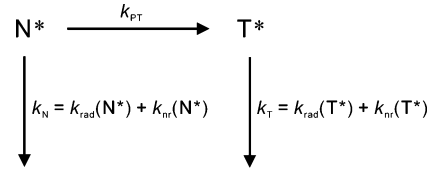

fluorescence lifetimes and their initial percent amplitudes at diverse values of w_0 by fitting fluorescence kinetics globally to biexponential functions (Table 3). Although the slow component changes more rapidly, both the fast and slow ones become fast with w_0 increase. We attribute these changes to shortened solvation times with w_0 (Figure 3 and Table 2). The additional contribution of the increased ESDPT rate is considered to change the slow component more rapidly with w_0 (vide infra). Table 4 shows that the decay times of the fast and the slow components indeed increase with the wavelength of monitored fluorescence as already discussed. Thus, we have extracted rate constants considering tautomeric fluorescence kinetics rather than a normal one to avoid the interference of solvation time changes.To understand the ESDPT dynamics of 7AI in the water nanopools of reverse micelles, we have analyzed the observed biexponential kinetic constants of tautomer fluorescence by employing the irreversible two-state model suggested to describe the relaxation of excited 7AI in water and alcohols.[17,18] The k_{rad} and k_{nr} of Scheme 2 denote the radiative- and the nonradiative-relaxation rate constants, respectively. Then, we can derive eqs 2 and 3 to show the temporal behaviors of [N*] and [T*], respectively

$$[N^*] = [N^*]_0 e^{-(k_N + k_{PT})t} \tag{2}$$

$$[T^*] = \left(\frac{[N^*]_0 k_{PT}}{k_N + k_{PT} - k_T}\right)[e^{-k_T t} - e^{-(k_N + k_{PT})t}] \tag{3}$$

Because k_T is assumed to be greater than ($k_N + k_{PT}$) as reported in bulk water,[18] the apparent rise time of eq 3 is represented by $(k_T)^{-1}$ while the apparent decay time by $(k_N + k_{PT})^{-1}$. The observation that the slow decay time of N* is the same as the

TABLE 5: Rate Constants and KIEs[a] Following the Two-State Model

w_0	isotope	k_{PT} (s^{-1})	KIE of k_{PT}	k_T (s^{-1})	KIE of k_T
4	^{1}H	5.6×10^8	2.7	1.7×10^9	2.0
	^{2}H	2.1×10^8		8.6×10^8	
8	^{1}H	7.2×10^8	2.8	2.0×10^9	2.0
	^{2}H	2.6×10^8		1.0×10^9	
16	^{1}H	8.4×10^8		2.4×10^9	
32	^{1}H	9.1×10^8	3.0	2.5×10^9	1.9
	^{2}H	3.0×10^8		1.3×10^9	
60	^{1}H	8.9×10^8		2.5×10^9	

[a] Average percent deviations in the replicate measurements of rate constants and KIEs are ±5% and ±7%, respectively.

decay time of T* indicates that the assumption is valid. The value of $(k_N)^{-1}$ was assumed to be 6.2 ns, which is the emission lifetime of 7AI in reverse micelles of $w_0 = 0$. On the other hand, that observed with the protic hydrogen of ^{2}H has been assumed to be 7.4 ns because the KIE of k_N for an ESDPT-blocked 7AI-derivative compound of N_1-methyl-7-azaindole is 1.2.[18]

The biexponential global fits of T* fluorescence kinetics yield rate constants and KIEs listed in Table 4. Both k_{PT} and KIE increase with w_0. However, they are significantly smaller even at $w_0 = 32$ than the respective values of $(1.1 \pm 0.1) \times 10^9$ s^{-1} and 4.0 ± 0.3 in bulk water, which have been deduced using the k_N of N_1-methyl-7-azaindole.[18] Because the dynamics of molecules in the free-water regions of reverse micelles is the same as that reported in bulk water, the above observations also support that 7AI molecules are present in the bound-water regions. Recall that the acid−base reaction kinetics of 2-naphthol derivatives is reported to depend on the residence site of the photoacids in reverse micelles.[57] Thus, the proton-transfer dynamics of 2-naphthol derivatives in the free-water regions remains invariant with $w_0 \geq 10$.[32,59,60] Note that the KIE of k_T changes hardly with w_0, although the value itself of k_T increases. This signifies that the above kinetic analysis is reliable.

Solvent-Assisted Proton Transfer of 7AI in Water Nanopools. The cyclically bridged structure depicted in Scheme 1, which is essential for facile ESDPT, is energetically unfavorable in water so that 7AI molecules are considered to have a wide range of H-bonded structures with water molecules.[19−21] The cyclic structure is disfavored in water owing to the disadvantageous angles and lengths of involved H-bonds and to the expense of an extensive H-bonded network involving external water molecules. Thus, only a small fraction of 7AI molecules possess the appropriate H-bonded configuration in water. Then, solvent reorganization to form the cyclic structure is presumed to be an important process in the proton transfer of photoexcited 7AI. The k_{PT} and the KIE of proton transfer increase with the size of the water nanopool in a reverse micelle (Table 5). Furthermore, their observed values remain to be significantly smaller than those in bulk water. These suggest that 7AI molecules are located in the bound-water regions surrounded by the charged headgroup layers of reverse micelles[29−31] and that they have an energetically and dynamically different environment from 7AI molecules in bulk water. The slow process in the solvation dynamics of biological water has been proposed to arise from a dynamic exchange between free and bound water molecules.[29−31,55,56] Along this picture, bound water molecules are suggested to undergo reorganization more slowly than free water molecules owing to the strong H-bonds with nearby charged headgroups of surfactant molecules. Water relays a proton via the formation of the cyclic geometry with H-bonding to 7AI during the tautomerization of photoexcited 7AI. Thus, the formation rate of the cyclic structure is suggested

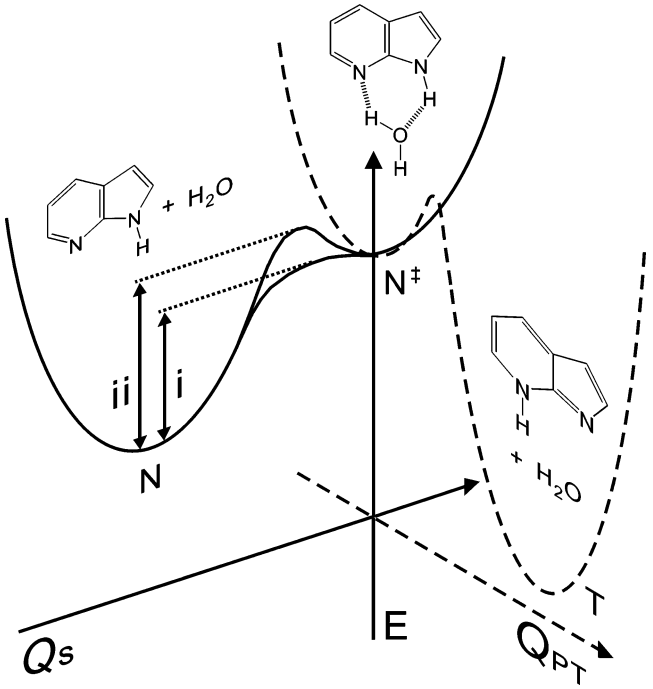

Figure 5. Schematic energetics for the two-step model of 7AI ESDPT in water. Q_S and Q_{PT} denote the coordinates of solvation and proton transfer, respectively, and **i** and **ii** denote $\Delta G^‡$ in bulk water and in AOT reverse micelles, respectively.

to control the dynamics of ESDPT. To correlate H-bond energetics with ESDPT dynamics, we adopt a continuous solvation model of $k_{PT} = k_{pt} \exp(-\Delta G^‡/k_B T)$, where $\Delta G^‡$ is the free energy of N‡ formation from N.[19] In this description, the intrinsic proton transfer of N‡ to form T is assumed to take place rapidly via tunneling or without a barrier.[24]

Consequently, solvent reorganization to form N‡ in the bound-water regions of reverse micelles becomes energetically less favorable than in bulk water to reduce the overall proton-transfer rate constant of 7AI. Moreover, the KIE of k_{PT} is also smaller in the bound-water regions than in bulk water because the rate of isotope-insensitive solvation is more influential to the overall rate of proton transfer.

The anomalous behavior of KIE that increases with temperature in bulk alcohols has been attributed to the shift of the rate-controlling step from the temperature-dependent and isotope-independent solvation process toward the temperature-independent and isotope-dependent intrinsic proton-transfer event in the overall proton transfer of 7AI.[17] The disruption of H-bonds to form N‡ is more difficult in the bound-water regions than in bulk water because 7AI and water molecules are tightly bound to the nearby headgroups of AOT molecules. This increases $\Delta G^‡$ to decrease k_{PT} and shifts the rate-determining step toward the solvation process to reduce KIE. The ESDPT dynamics of 7AI in the water nanopools of reverse micelles is shown schematically in Figure 5. Note that the excited-state tautomerization process of 7AI in the core regions of methanol reverse micelles is recently reported to become faster than that in bulk methanol due to a constrained H-bonded network among methanol molecules.[64] The increased rate in methanol reverse micelles has been attributed to the reduction of $\Delta G^‡$, which renders the overall rate constant and the KIE of ESDPT larger than the respective values in bulk methanol.

In summary, 7AI molecules in the water nanopools of AOT reverse micelles are found to locate at the bound-water regions. The k_{PT} and the KIE of proton transfer are smaller in reverse

micelles than in bulk water, although both increase with the size of the water pool. The retardation of proton transfer in the bound-water regions is attributed to the increased free energy of solvation to form a prerequisite cyclically bridged 1:1 7AI/water complex. Isotope-insensitive solvation becomes more rate-determining to show smaller KIEs in reverse micelles than in bulk water.

Acknowledgment. The Korea Research Foundation is appreciated for the grant of KRF-2004-015-C00230. D.-J.J. and O.-H.K. also thank the Strategic National R&D and the Brain Korea 21 Programs, respectively.

References and Notes

(1) Tanner, C.; Manca, C.; Leutwyler, S. *Science* **2003**, *302*, 1736.

(2) Rini, M.; Magnes, B.-Z.; Pines, E.; Nibbering, E. T. *Science* **2003**, *301*, 349.

(3) Geissler, P. L.; Dellago, C.; Chandler, D.; Hutter, J.; Parrinello, M. *Science* **2001**, *291*, 2121.

(4) Douhal, A.; Kim, S. K.; Zewail, A. H. *Nature* **1995**, *378*, 260.

(5) Watson, J. D.; Crick, F. H. C. *Nature* **1953**, *171*, 964.

(6) (a) Abou-Zied, O. K.; Jimenez, R.; Romesberg, F. E. *J. Am. Chem. Soc.* **2001**, *123*, 4613. (b) Ogawa, A. K.; Abou-Zied, O. K.; Tsui, V.; Jimenez, R.; Case, D. A.; Romesberg, F. E. *J. Am. Chem. Soc.* **2000**, *122*, 9917.

(7) (a) Taylor, C. A.; El-Bayoumi, M. A.; Kasha, M. *Proc. Natl. Acad. Sci. U.S.A.* **1969**, *63*, 253. (b) Ingham, K. C.; Abu-Elgheit, M.; El-Bayoumi, M. A. *J. Am. Chem. Soc.* **1971**, *93*, 5023. (c) Ingham, K. C.; El-Bayoumi, A. *J. Am. Chem. Soc.* **1974**, *96*, 1674.

(8) (a) Fiebig, T.; Chachisvilis, M.; Manger, M.; Zewail, A. H.; Douhal, A.; Garcia-Ochoa, I.; de La Hoz Ayuso, A. *J. Phys. Chem. A* **1999**, *103*, 7419. (b) Chachisvilis, M.; Fiebig, T.; Douhal, A.; Zewail, A. H. *J. Phys. Chem. A* **1998**, *102*, 669.

(9) (a) Catalán, J.; Perez, P.; del Valle, J. C.; de Paz, J. L. G.; Kasha, M. *Proc. Natl. Acad. Sci. U.S.A.* **2002**, *99*, 5793. (b) Catalán, J.; del Valle, J. C.; Kasha, M. *Proc. Natl. Acad. Sci. U.S.A.* **1999**, *96*, 8338. (c) Catalán, J.; Kasha, M. *J. Phys. Chem. A* **2000**, *104*, 10812.

(10) Folmer, D. E.; Wisniewski, E. S.; Hurley, S. M.; Castleman, A. W., Jr. *Proc. Natl. Acad. Sci. U.S.A.* **1999**, *96*, 12980.

(11) (a) Takeuchi, S.; Tahara, T. *Chem. Phys. Lett.* **2001**, *347*, 108. (b) Takeuchi, S.; Tahara, T. *J. Phys. Chem. A* **1998**, *102*, 7740. (c) Takeuchi, S.; Tahara, T. *Chem. Phys. Lett.* **1997**, *277*, 340.

(12) (a) Chou, P.-T.; Liao, J.-H.; Wei, C.-Y.; Yang, C.-Y.; Yu, W.-S.; Chou, Y.-H. *J. Am. Chem. Soc.* **2000**, *122*, 986. (b) Yu, W.-S.; Cheng, C.-C.; Chang, C.-P.; Wu, G.-R.; Hsu, C.-H.; Chou, P.-T. *J. Phys. Chem. A* **2002**, *106*, 8006.

(13) (a) Sakota, K.; Sekiya, H. *J. Phys. Chem. A* **2005**, *109*, 2718. (b) Sakota, K.; Sekiya, H. *J. Phys. Chem. A* **2005**, *109*, 2722. (c) Sakota, K.; Okabe, C.; Nishi, N.; Sekiya, H. *J. Phys. Chem. A* **2005**, *109*, 5247.

(14) (a) Smirnov, A. V.; English, D. S.; Rich, R. L.; Lane, J.; Teyton, L.; Schwabacher, A. W.; Luo, S.; Thornburg, R. W.; Petrich, J. W. J. *Phys. Chem. B* **1997**, *101*, 2758. (b) Negrerie, M.; Gai, F.; Bellefeuille, S. M.; Petrich, J. W. *J. Phys. Chem.* **1991**, *95*, 8663. (c) Negrerie, M.; Gai, F.; Lambry, J. C.; Martin, J. L.; Petrich, J. W. *J. Phys. Chem.* **1993**, *97*, 5046.

(15) Konijnenberg, J.; Huizer, A. H.; Varma, C. A. G. O. *J. Chem. Soc., Faraday Trans. 2* **1988**, *84*, 1163.

(16) Moog, R. S.; Bovino, S. C.; Simon, J. D. *J. Phys. Chem.* **1988**, *92*, 6545.

(17) Moog, R. S.; Maroncelli, M. *J. Phys. Chem.* **1991**, *95*, 10359.

(18) Chapman, C. F.; Maroncelli, M. *J. Phys. Chem.* **1992**, *96*, 8430.

(19) Mente, S.; Maroncelli, M. *J. Phys. Chem. A* **1998**, *102*, 3860.

(20) Waluk, J. *Acc. Chem. Res.* **2003**, *36*, 832.

(21) Kyrychenko, A.; Stepanenko, Y.; Waluk, J. *J. Phys. Chem. A* **2000**, *104*, 9542.

(22) Chou, P.-T.; Yu, W.-S.; Wei, C.-Y.; Cheng, Y.-M.; Yang, C.-Y. *J. Am. Chem. Soc.* **2001**, *123*, 3599.

(23) Chou, P. T.; Martinez, M. L.; Cooper, W. C.; Collins, S. T.; McMorrow, D. P.; Kasha, M. *J. Phys. Chem.* **1992**, *96*, 5203.

(24) Kwon, O.-H.; Lee, Y.-S.; Park, H. J.; Kim, Y.; Jang, D.-J. *Angew. Chem., Int. Ed.* **2004**, *43*, 5792.

(25) (a) Chen, Y.; Gai, F.; Petrich, J. W. *J. Am. Chem. Soc.* **1993**, *115*, 10158. (b) Gai, F.; Chen, Y.; Petrich, J. W. *J. Am. Chem. Soc.* **1992**, *114*, 8343. (c) Chen, Y.; Rich, R. L.; Gai, F.; Petrich, J. W. *J. Phys. Chem.* **1993**, *97*, 1770.

(26) (a) Moreno, M.; Douhal, A.; Lluch, J. M.; Castano, O.; Frutos, L. M. *J. Phys. Chem. A* **2001**, *105*, 3887. (b) Douhal, A.; Moreno, M.; Lluch, J. M. *Chem. Phys. Lett.* **2000**, *324*, 75. (c) Douhal, A.; Moreno, M.; Lluch, J. M. *Chem. Phys. Lett.* **2000**, *324*, 81. (d) Douhal, A.; Guallar, V.; Moreno, M.; Lluch, J. M. *Chem. Phys. Lett.* **1996**, *256*, 370.

(27) Ray, J. G.; Sengupta, P. K. *Chem. Phys. Lett.* **1994**, *230*, 75.

(28) Ashenhurst, J.; Wu, G.; Wang, S. *J. Am. Chem. Soc.* **2000**, *122*, 2541.

(29) Bhattacharyya, K. *Acc. Chem. Res.* **2003**, *36*, 95.

(30) Nandi, N.; Bhattacharyya, K.; Bagchi, B. *Chem. Rev.* **2000**, *100*, 2013.

(31) Bhattacharyya, K.; Bagchi, B. *J. Phys. Chem. A* **2000**, *104*, 10603.

(32) Cohen, B.; Huppert, D.; Solntsev, K. M.; Tsfadia, Y.; Nachliel, E.; Gutman, M. *J. Am. Chem. Soc.* **2002**, *124*, 7539.

(33) Kalyanasundaram, K. *Photochemistry in Microheterogeneous Systems*; Academic Press: Orlando, FL, 1987; Chapter 5.

(34) Hirose, Y.; Yui, H.; Sawada, T. *J. Phys. Chem. B* **2004**, *108*, 9070.

(35) Correa, N. M.; Zorzan, D. H.; Chiarini, M.; Cerichelli, G. *J. Org. Chem.* **2004**, *69*, 8224.

(36) Hazra, P.; Chakrabarty, D.; Chakraborty, A.; Sarkar, N. *J. Photochem. Photobiol., A* **2004**, *167*, 23.

(37) Raju, B. B.; Costa, S. M. B. *J. Phys. Chem. B* **1999**, *103*, 4309.

(38) Datta, A.; Mandal, D.; Pal, S. K.; Bhattacharyya, K. *J. Phys. Chem. B* **1997**, *101*, 10221.

(39) Mukherjee, L.; Mitra, N.; Bhattacharyya, P. K.; Moulik, S. P. *Langmuir* **1995**, *11*, 2866.

(40) Maitra, A. *J. Phys. Chem.* **1984**, *88*, 5122.

(41) Hauser, H.; Haering, G.; Pande, A.; Luisi, P. L. *J. Phys. Chem.* **1989**, *93*, 7869.

(42) Venables, D. S.; Huang, K.; Schmuttenmaer, C. A. *J. Phys. Chem. B* **2001**, *105*, 9132.

(43) Moran, P. D.; Bowmaker, G. A.; Cooney, R. P.; Bartlett, J. R.; Woolfrey, J. L. *Langmuir* **1995**, *11*, 738.

(44) Onori, G.; Santucci, A. *J. Phys. Chem.* **1993**, *97*, 5430.

(45) Jain, T. K.; Varshney, M.; Maitra, A. *J. Phys. Chem.* **1989**, *93*, 7409.

(46) D'Aprano, A.; Lizzio, A.; Liveri, V. T.; Aliotta, F.; Vasi, C.; Migliardo, P. *J. Phys. Chem.* **1988**, *92*, 4436.

(47) Dutta, P.; Sen, P.; Mukherjee, S.; Halder, A.; Bhattacharyya, K. *J. Phys. Chem. B* **2003**, *107*, 10815.

(48) Sen, S.; Dutta, P.; Sukul, D.; Bhattacharyya, K. *J. Phys. Chem. A* **2002**, *106*, 6017.

(49) Pal, S. K.; Mandal, D.; Sukul, D.; Bhattacharyya, K. *Chem. Phys. Lett.* **1999**, *312*, 178.

(50) Sarkar, N.; Das, K.; Datta, A.; Das, S.; Bhattacharyya, K. *J. Phys. Chem.* **1996**, *100*, 10523.

(51) (a) Hazra, P.; Chakrabarty, D.; Sarkar, N. *Chem. Phys. Lett.* **2003**, *371*, 553. (b) Hazra, P.; Chakrabarty, D.; Sarkar, N. *Langmuir* **2002**, *18*, 7872.

(52) Riter, R. E.; Willard, D. M.; Levinger, N. E. *J. Phys. Chem. B* **1998**, *102*, 2705.

(53) Mittleman, D. M.; Nuss, M. C.; Colvin, V. L. *Chem. Phys. Lett.* **1997**, *275*, 332.

(54) Abel, S.; Sterpone, F.; Bandyopadhyay, S.; Marchi, M. *J. Phys. Chem. B* **2004**, *108*, 19458.

(55) Balasubramanian, S.; Pal, S.; Bagchi, B. *Phys. Rev. Lett.* **2002**, *89*, 115505.

(56) Nandi, N.; Bagchi, B. *J. Phys. Chem. B* **1997**, *101*, 10954.

(57) Faeder, J.; Ladanyi, B. *J. Phys. Chem. B* **2001**, *105*, 11148.

(58) (a) Pal, S. K.; Zewail, A. H. *Chem. Rev.* **2004**, *104*, 2099. (b) Pal, S. K.; Peon, J.; Bagchi, B.; Zewail, A. H. *J. Phys. Chem. B* **2002**, *106*, 12376. (c) Peon, J.; Pal, S. K.; Zewail, A. H. *Proc. Natl. Acad. Sci. U.S.A.* **2002**, *99*, 10964. (d) Kamal, J. K. A.; Zhao, L.; Zewail, A. H. *Proc. Natl. Acad. Sci.* **2004**, *101*, 13411. (e) Zhao, L.; Pal, S. K.; Xia, T.; Zewail, A. H. *Angew. Chem., Int. Ed.* **2003**, *43*, 60.

(59) (a) Escabi-Perez, J. R.; Fendler, J. H. *J. Am. Chem. Soc.* **1978**, *100*, 2234. (b) Politi, M. J.; Brandt, O.; Fendler, J. H. *J. Phys. Chem.* **1985**, *89*, 2345. (c) Politi, M. J.; Chaimovich, H. *J. Phys. Chem.* **1986**, *90*, 282.

(60) (a) Bardez, E.; Monnier, E.; Valeur, B. *J. Phys. Chem.* **1985**, *89*, 5031. (b) Bardez, E.; Goguillon, B.-T.; Keh, E.; Valeur, B. *J. Phys. Chem.* **1984**, *88*, 1909.

(61) (a) Meech. S. R.; Phillis, D.; Lee, A. G. *Chem. Phys.* **1983**, *80*, 317. (b) Ashby, K. D.; Das, K.; Petrich, J. W. *Anal. Chem.* **1997**, *69*, 1925. (c) Rich, R. L.; Chen, Y.; Neven, D.; Négrerie, M.; Gai, F.; Petrich, J. W. *J.* Phys. Chem. **1993**, *97*, 1781. (d) Tubergen, M. J.; Levy, D. H. *J. Phys. Chem.* **1991**, *95*, 2175. (e) Demmer, D. R.; Leach, G. W.; Outhouse, E. A.; Hager, J. W.; Wallace, S. C. *J. Phys. Chem.* **1990**, *94*, 82.

(62) Maroncelli, M.; Fleming, G. R. *J. Chem. Phys.* **1987**, *86*, 6221.

(63) Cho, C. H.; Chung, M.; Lee, J.; Nguyen, T.; Singh, S.; Vedamuthu, M.; Yao, S.; Zhu, J.-B.; Robinson, G. W. *J. Phys. Chem.* **1995**, *99*, 7806.

(64) Kwon, O.-H.; Jang, D.-J. *J. Phys. Chem. B* **2005**, *109*, 8049.